

## Recent precipitation trends and future scenarios over the Mediterranean Sea

*Mohamed Shaltout<sup>1</sup> and Anders Omstedt<sup>2</sup>*

<sup>1</sup> University of Alexandria, Faculty of Science, Department of Oceanography, Alexandria, Egypt

<sup>2</sup> University of Gothenburg, Department of Earth Sciences, Gothenburg, Sweden

*Received 13 May 2014, in final form 19 September 2014*

This paper analyses current precipitation rates (PRs) and trends over the Mediterranean Sea region and their response to global climate change scenarios. The analysis uses 0.25° gridded PRs dataset over a 13-year period (1998–2010) based on remote sensing data from the Tropical Rainfall Measuring Mission. Future scenarios use the results of six global climate models (GCMs) under four representative concentration pathway scenarios (i.e., RCP26, RCP45, RCP60, and RCP85).

Results indicate that the Mediterranean Sea region displays a seasonally significant (insignificant) wetter trend during cold (hot) seasons, and exhibits annual spatial variation ranging from under 15 to over 100 mm month<sup>-1</sup> over the period 1998–2010. Sea level pressure has two different effects on precipitation over the northern (inversely related to precipitation) versus southern (directly related to precipitation) Mediterranean Sea. However, sea surface temperature is anti-correlated with precipitation. The GCMs that describe the current Mediterranean Sea precipitation most realistically are GFDL-CM3-1, MIROC-ESM-CHEM, and HadGEM2-AO, which are used to calculate the ensemble mean for each representative concentration pathway scenario. The ensemble means realizations indicate that the study area will experience substantial drought in the 21<sup>st</sup> century. Uncertainty in the projected precipitation over the Mediterranean Sea was partitioned into four sources, of which the used scenario dominates.

*Keywords:* Mediterranean Sea, Black Sea, precipitation, climate models

### 1. Introduction

The Mediterranean Sea (Fig. 1), which extends from  $-7^{\circ}$  to  $36^{\circ}$  east and  $30^{\circ}$  to  $46^{\circ}$  north, represents a significant resource for tourism, oil, and gas extraction, fishing, farming, and trade. The Mediterranean region has undergone large cli-

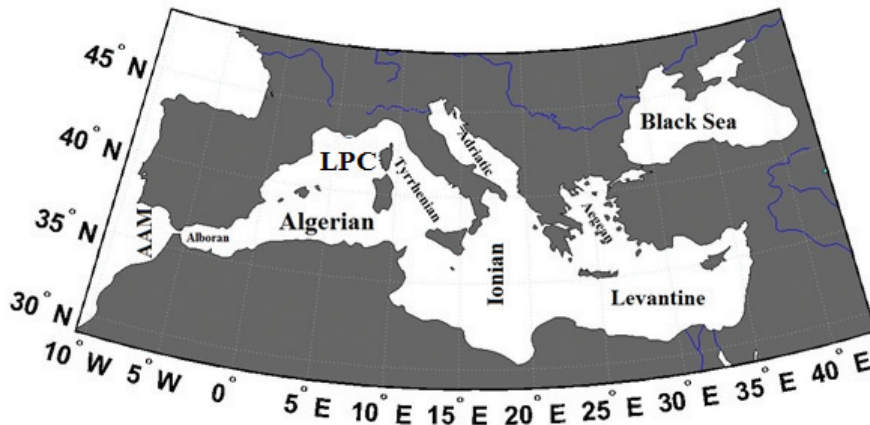


**Figure 1.** The Mediterranean and adjacent sub-basins (LPC = Liguro–Provençal and Catalan sub-basins, AAM = Active Atlantic Mediterranean sub-basin west of the Strait of Gibraltar).

mate change in the past (Lionello et al., 2006b) and might be a climate change hot-spot in the future due to the global warming associated with increasing greenhouse gas concentrations (Lionello et al., 2006a; Giorgi and Lionello, 2008).

The Mediterranean Sea is characterized by wet winters and dry summers. Xoplaki (2002) defined the Mediterranean wet season as extending from October to March, but with considerable variability in precipitation rates (PRs). Hurrell (1995), Mariotti et al. (2002) and Romanou et al. (2010) found that the winter North Atlantic Oscillation (NAO) is anti-correlated with precipitation, especially over the western and northern–central Mediterranean regions. Following Xoplaki et al. (2004), we regard the Mediterranean Sea wet season as controlled by the atmospheric large-scale circulation represented by sea level pressure, though sea surface temperature (SST) also has a small effect. Dry summers are due to high sea level pressure when atmospheric subsidence dominates over the Mediterranean region (Giorgi and Lionello, 2008).

Trenberth and Shea (2005) showed that the drier condition of the Mediterranean Sea associated with warmer conditions. Mariotti and Dell’Aquila (2012) support the previous findings and showed that the sea surface temperature rise is combined with decrease in precipitation rates over the Mediterranean Sea. Moreover, Berg et al. (2013) showed that the connective precipitation increase with increased temperature. In addition, they did not find that the heavy stratiform precipitation is linked to high temperature. Recently, Shaltout and Omstedt (2014) found that the annual Mediterranean Sea precipitation is in strongly negative correlation with sea surface temperature.

Henry (1977) and Kjellström et al. (2011) noticed that the Mediterranean Sea is characterized by maximal (minimal) PRs over the European (African)

coasts. The Alpine chain is considered as an important source of moisture for the northern Mediterranean Region (Lionello et al., 2006a,b). Precipitation south of the Alps is controlled by the large-scale atmospheric circulation represented by sea level pressure (Efthymiadis et al., 2007). Following Bordi and Sutera (2008), the Mediterranean Sea experienced severe dry/wet events during the 2000–2007 period, while north-western Africa and central Europe (including central–southern Italy) experienced a high percentage of dry (wet) events during the same period.

Mariotti et al. (2002) estimated several PRs using different datasets for the 1979–1993 period, estimating that the Mediterranean Sea has annual mean precipitation ranging from 27.5 to 40 mm month<sup>-1</sup>. Romanou et al. (2010) estimated PRs during the 1988–2005 period over the Mediterranean Sea based on satellite-derived ocean fluxes (HOAPS-3 satellite data) and found a range of 6–60 mm month<sup>-1</sup>, more (less) pronounced over the northern Ionian sub-basin and western Black Sea (eastern and southern Mediterranean Sea). Shaltout and Omstedt (2012) estimated that the annual average PR over the eastern Mediterranean Sea during the 1958–2009 period was 48 mm month<sup>-1</sup>, with the highest rates in December (i.e., 98 mm month<sup>-1</sup>). Precipitation occurs mainly in the cold months over the southern Mediterranean region; however, over the northern Mediterranean region, significant precipitation occurs in all seasons (Kelley et al., 2012).

According to the recent IPCC (2013) assessment, the Mediterranean Sea is projected to experience a significant drying trend associated with increasing sea surface temperature until 2100. Giorgi and Lionello (2008) projected a pronounced drying (–25% to –30%) in the current century for the Mediterranean region, most markedly in summer. Their analysis used coupled atmosphere–ocean general circulation models forced using the ensemble mean of 17 global climate models (GCMs). Romanou et al. (2010) demonstrated that the central Mediterranean, eastern Mediterranean, and Black Sea (western Mediterranean Sea) experienced a drying (wetting) trend of –0.6, –0.3, and –6 mm month<sup>-1</sup> yr<sup>-1</sup> (3 mm month<sup>-1</sup> yr<sup>-1</sup>), respectively, over the 1988–2005 period. Kjellström et al. (2011) stated that the Mediterranean Sea region will experience increased drought by the end of the current century based on scenario A1B. Shaltout and Omstedt (2012) demonstrated that the eastern Mediterranean Sea experienced a drying trend of 0.06 mm month<sup>-1</sup> yr<sup>-1</sup> over the 1958–2009 period. The expected drying trends in the Mediterranean Sea are not uniformly distributed, as there are sub-areas where wetting trends are also expected, for example, the Alps region especially in winter (Giorgi and Lionello, 2008) and some sub-regions in the south and east (Jacobeit et al., 2007).

New spatial and temporal precipitation trends over the Mediterranean Sea were further studied using reanalysed data (Mariotti et al., 2002; Shaltout and Omstedt, 2012), downscaled global climate modelling (Giorgi and Lionello, 2008), and HOAPS-3 satellite data (Romanou et al., 2010). The present study follows such

recent work but uses new remote sensing data from the Tropical Rainfall Measuring Mission (TRMM) and separates the Mediterranean Sea into ten sub-basins. In addition, this work analyses projected Mediterranean precipitation patterns and trends using the more recent scenarios (CMIP5, the Coupled Model Intercomparison Project 5). CMIP5 gives better resolution and dynamics than do the previous-generation CMIP3 multi-model ensembles (Taylor et al., 2012), resulting in improved estimates of the average PRs and trends for the Mediterranean region.

We use a 13-year high-resolution precipitation database: 1) to examine the spatial and temporal variability of precipitation over the Mediterranean Sea and its surrounding sub-basins; 2) to examine the relationship between precipitation in the study area and other atmospheric parameters, such as the North Atlantic Oscillation Index (NAOI), mean sea level pressure (SLP), and sea surface temperatures (SST); and 3) to examine projected precipitation over the study area up to 2100 using six GCMs with the most recent projection scenarios. The materials and methods used are presented in Section 2, the results in Section 3, and the discussion and conclusions in Section 4.

## 2. Materials and methods

### 2.1. Materials used

This paper analyses the present characteristics and future trends and uncertainties of PRs over the Mediterranean Sea based on various available data sources, as follows.

- **Precipitation data:** Gridded three-hour Tropical Rainfall Measuring Mission (TRMM) data with a  $0.25^\circ$  spatial grid (version 6), 1998–2010, were used to study recent precipitation characteristics. TRMM is part of NASA’s mission to monitor and study tropical rainfall in cooperation with the Japan Aerospace Exploration Agency using TRMM and other satellite precipitation products. TRMM (version 6) merges high-quality microwave precipitation estimates when available and calibrated infrared precipitation estimates otherwise (full algorithms are available at <http://trmm.gsfc.nasa.gov/3b42.html>). TRMM data are considered the most effective tools for estimating the PR at the nominal observation time (Huffman et al., 2007; Gopalan et al., 2010).
- **Atmospheric data:** Daily NAOI data were extracted from the KNMI Climate Explorer website for the 1998–2010 period. Gridded daily sea level pressure (SLP) data were extracted from the ERA-Interim full-resolution ( $0.75^\circ \times 0.75^\circ$ ) database for the same period. Gridded daily AVHRR SST data (version 2) with a  $0.25^\circ$  latitude/longitude spatial grid were also extracted. The data were used to study recent statistical correlations between precipitation and various atmospheric components, such as NAO, SLP, and SST.

– **Future precipitation data:** Model output from six GCMs using four 21<sup>st</sup>-century CMIP5 scenarios (i.e., RCP26, RCP45, RCP60, and RCP85) were used (Tab. 1). RCP stands for “Representative Concentration Pathways” and the following number indicates one tenth of the assumed radiative forcing at the end of the 21<sup>st</sup> century. These data were used to study future expected precipitation rates and trends, and the deviations between the best models were used as a measure of model uncertainty.

## 2.2. Methodology

The TRMM dataset is used to describe the spatial and temporal variability of precipitation over the Mediterranean and adjacent sub-basins and to evaluate how the GCMs used describe the current precipitation structure. Based on this

*Table 1. Simulation of various global climate models following the CMIP5 protocol with four projected future Representative Concentration Pathway (RCP) scenario*

Model (number of realizations for each scenario)	Organization group	Simulation period	Spatial resolution °lat × °lon (relevant source)
GFDL-CM3 (1)	Geophysical Fluid Dynamics Laboratory, Coupled Physical Model; National Oceanic and Atmospheric Administration (NOAA) <b>USA</b>	From historical conditions (1860–2005) up to 2300	2.0° × 2.5° (Donner et al., 2011)
bcc-csm1-1 (1)	Beijing Climate Center: Climate System Model for the last century <b>China</b>	From historical conditions (1850–2005) up to 2300	2.8° × 2.8° (Tongwen et al., 2013)
MRI-CGCM3 (1)	Meteorological Research Institute. <b>Japan</b>	From historical conditions (1850–2005) up to 2100	1.125° × 1.125° (Yukimoto et al., 2011)
MIROC-ESM- CHEM (1)	Japan Agency for Marine-Earth Science and Technology; Atmosphere and Ocean Research Institute (The University of Tokyo); National Institute for Environmental Studies. <b>Japan</b>	From historical conditions (1850–2005) up to 2100	2.8° × 2.8° (Watanabe et al., 2011)
HadGEM2-AO (1)	National Institute of Meteorological Research/Korea Meteorological Administration. <b>Korea</b>	From historical conditions (1860–2005) up to 2100	1.25° × 1.875° (Baek et al., 2013)
CCSM4 (6)	National Center for Atmospheric Research; National Center for Atmospheric Research (NCAR) <b>USA</b>	From historical conditions (1850–2005) up to 2300	1.00° × 1.25° (Gent et al., 2011)

evaluation, a mini-ensemble mean realization is calculated for each RCP scenario based on the GCMs that realistically describe the current precipitation conditions.

### 2.2.1. TRMM precipitation dataset

The spatial and temporal distributions of precipitation over the Mediterranean and adjacent regions are studied using the TRMM three-hour dataset over a 13-year period focusing on seasonal and inter-annual variability. Linear trends for each grid, each sub-basin, and the entire study area are calculated using ordinary least squares estimation.

The annual precipitation range is defined as the difference between the maximum and minimum precipitation throughout the study period at each grid point (Chu and Lan, 2012). This definition calculates the exact precipitation range, avoiding the effects of annual shifts of wet and dry seasons. However, this definition might not give the exact annual precipitation range, especially in areas characterized by marked seasonal and annual variation (e.g., the Mediterranean Sea). This method might be unsuitable for describing the annual precipitation range of the study area, so the current research instead calculates the annual precipitation range ( $P_{an}(i, j)$ ) at each grid point ( $i, j$ ) using seasonal averages in the following formula:

$$P_{an}(i, j) = \frac{\sum_{yr=1}^{yr=N} (\text{seasonal maximum}(i, j) - \text{seasonal minimum}(i, j))}{N} \quad (1)$$

where  $N$  is number of years studied and equal to 13.

The study area, i.e., the Mediterranean Sea and adjacent sub-basins (hereafter called Med+), is divided into ten sub-basins: the Active Atlantic Mediterranean (west of Gibraltar Strait; hereafter, AAM), Alboran, Algerian, Tyrrhenian, Liguro-Provençal and Catalan (hereafter, LPC), Ionian, Levantine, Aegean, Adriatic, and Black Sea sub-basins. These sub-basins are illustrated in Fig. 1.

The average number of very wet days is calculated and analysed for each sub-basin on annual and seasonal bases. A very wet day is defined as a day when the precipitation exceeds the sum of the mean of the entire Mediterranean precipitation and one standard deviation from the mean. Finally, daily correlation coefficients ( $R$ ) between precipitation and the other studied atmospheric parameters (i.e., NAO, SST, and SLP) are calculated on annual and seasonal bases. All the linear trends and correlation coefficients have been tested for significance by  $t$ -testing at the 95% level.

### 2.2.2. Global climate model results

The results of the six GCMs under the four RCP scenarios for the 1998–2010 period were examined using the TRMM precipitation dataset. The bias percent-

age (i.e.,  $100 \times \frac{\text{GCM} - \text{TRMM PR}}{\text{TRMM PR}} \%$ ) is used to test the performance of GCMs in simulating PRs over the study area (Kjellström et al., 2011; Shaltout et al., 2013). Only the GCMs that realistically describe the current climate precipitation conditions were used to calculate the mini-ensemble mean realization for each scenario.

The RCP scenarios include a low-forcing scenario (RCP26), two moderate-forcing stabilization scenarios (RCP45 and RCP60), and a high-forcing scenario (RCP85), as explained by Taylor et al. (2012) and Shaltout and Omstedt (2014).

To better understand the projected precipitation in the study area during the 21st century, uncertainties in the projection are analysed. In the current research, at least four sources of uncertainty are associated with the scenario design, the GCM itself as well as seasonal and regional variations. The source of the uncertainty is calculated only with respect to the GCMs used when calculating the mini-ensemble means. The contribution of each uncertainty source is determined using the range between the various simulations used.

### 3. Results

#### *3.1. Spatial and temporal distribution of precipitation over the Mediterranean and adjacent regions*

To characterize the total precipitation over the Med+ region, we calculate, based on 13-year data, the seasonal and annual average PRs. The annual average PRs over the study area ranged from 3.6 to 133.46 mm month<sup>-1</sup> and displayed a spatial distribution with increasing values towards the north and west and a spatially averaged variability of  $41.5 \pm 596$  mm month<sup>-1</sup> (Fig. 2a). The very wet area (mean Mediterranean precipitation plus 0.6 of standard deviation from the mean, 766 mm month<sup>-1</sup>) occurred only over 4% of the study area and only over the eastern Black Sea. The very dry area (mean Mediterranean precipitation minus 0.3 of standard deviation from the mean (236 mm month<sup>-1</sup>)) occurred only over 16% of the study period, especially over the southern part of the Levantine sub-basin. In general, the annual average PR over the northern Ionian sub-basin is much higher than over the Aegean sub-basin, which both are sub-basins at the same latitude. This is in accordance with the findings of Shaltout and Omstedt (2014), indicating that the Aegean sub-basin is colder than the northern Ionian sub-basin. In addition, precipitation over open water is higher than over coastal areas, indicating a stronger marine influence.

The annual average precipitation over the Med+ region differs significantly from season to season, being  $49 \pm 666$  mm month<sup>-1</sup> in winter,  $24 \pm 386$  mm month<sup>-1</sup> in spring,  $21 \pm 356$  mm month<sup>-1</sup> in summer, and  $102 \pm 1026$  mm month<sup>-1</sup> in autumn. In autumn, approximately 42% of the study area is considered very wet, especially over the central western Mediterranean, central Tyrrhenian, north

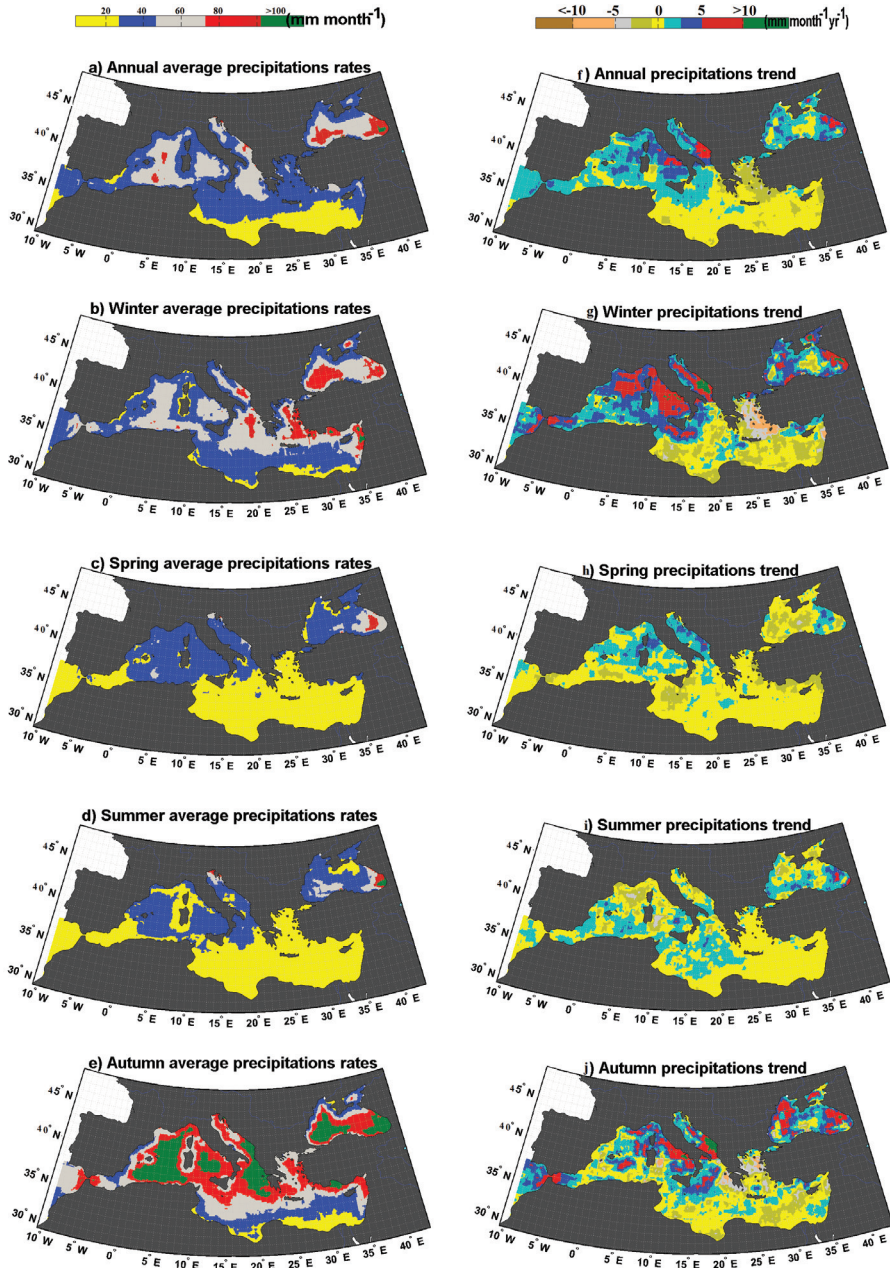


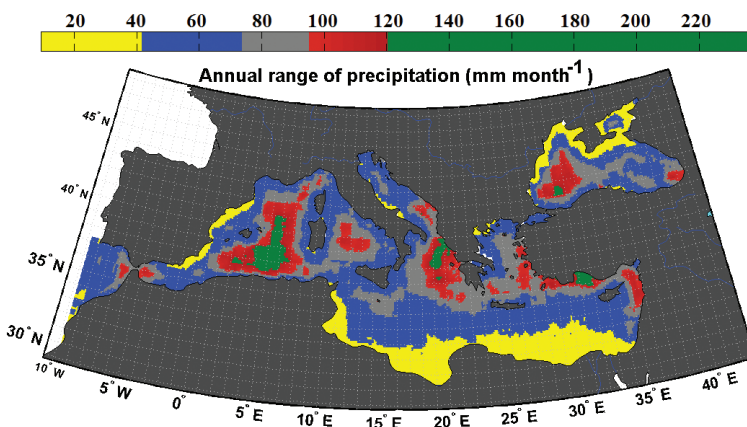
**Figure 2.** Spatial distribution of annual/seasonal precipitation rates, means, and trends over the 1998–2010 period in the Mediterranean and adjacent sub-basins; green in the left (right) panel indicates very wet areas (strong wetting trend), while yellow represents very dry areas (non-significant precipitation trend) of the Mediterranean Sea.

Ionian, and south Adriatic sub-basins together with the southern Black Sea (Fig. 2e). In winter, approximately 9% of the study area is considered very wet, especially over the Aegean sub-basin and southern Black Sea (Fig. 2b). In spring and summer, under 1% of the study area is considered very wet, especially over the southern part of the eastern Black Sea (Figs. 2c and 2d).

Approximately 43% of the Med+ region displayed non-significant precipitation trends, most markedly over the eastern Mediterranean sub-basin, as seen in Fig. 2f. In addition, strong wetting trends (greater than  $6 \text{ mm month}^{-1} \text{ yr}^{-1}$ ) were found over 2% of the Med+ region, especially over the south Adriatic sub-basin, central Tyrrhenian sub-basin, and eastern Black Sea. Moreover, only 6% of Med+ region displayed significant drying trends (less than  $1 \text{ mm month}^{-1} \text{ yr}^{-1}$ ), especially over the Aegean sub-basin.

Long-term (1989–2010) annually averaged precipitation trends over the Med+ region were  $1.14 \pm 1.6 \text{ mm month}^{-1} \text{ yr}^{-1}$ , peaking in winter ( $1.34 \pm 3.2 \text{ mm month}^{-1} \text{ yr}^{-1}$ ) and autumn ( $1.32 \pm 2.8 \text{ mm month}^{-1} \text{ yr}^{-1}$ ) as seen in Figs. 2g and 2j. In warm seasons, the average long-term precipitation trends over the area were insignificant (Figs. 2h and 2i).

In the Med+ region, the average annual precipitation range was calculated to be  $67 \pm 26 \text{ mm month}^{-1}$ , as seen in Fig. 3. The Med+ region reach their minimum annual range (under  $40 \text{ mm month}^{-1}$ ) over 16% of their area, especially along the Egyptian–Libyan Mediterranean coast, and reach their maximum annual range (over  $95 \text{ mm month}^{-1}$ ) over 15% of their area, especially over the central western Mediterranean sub-basin, northern Ionian sub-basin, western Black Sea, and offshore of Antalya, Turkey.



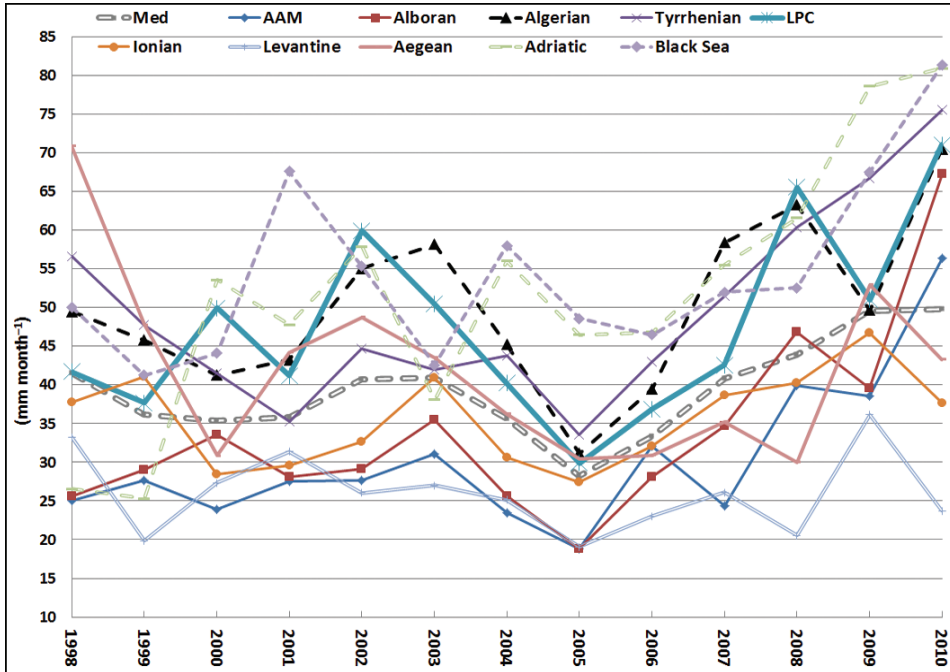
**Figure 3.** Spatial distribution of annual precipitation range over the 1998–2010 period in the Mediterranean Sea and adjacent sub-basins.

Table 2. Annual and seasonal precipitation rates characteristic of the studied sub-basins based on six-hour data from 1998 to 2010; *t*-test at a 95% significance level was used to test the linear trends. (Med = only the Mediterranean Sea).

	Annual trend (mm month <sup>-1</sup> yr <sup>-1</sup> )					Average $\pm$ standard deviation (mm month <sup>-1</sup> )				
	Annual					Annual				
	Winter	Spring	Summer	Autumn		Winter	Spring	Summer	Autumn	
Med	1.053	Non-significant	Non-significant	0.953		47.7 $\pm$ 72	21.2 $\pm$ 42	17.5 $\pm$ 37	71.07 $\pm$ 81	39.38 $\pm$ 65
Active Atlantic Mediterranean	2.896	Non-significant	Non-significant	2.930		42.2 $\pm$ 185	13.9 $\pm$ 77	5.7 $\pm$ 44	60.3 $\pm$ 212	30.52 $\pm$ 149.04
Alboran	4.105	Non-significant	Non-significant	3.377		45.9 $\pm$ 203	19.8 $\pm$ 132	7.8 $\pm$ 65	62.7 $\pm$ 257	34.02 $\pm$ 180.84
Algerian	2.201	Non-significant	Non-significant	1.256		45.9 $\pm$ 137	32.4 $\pm$ 113	23.7 $\pm$ 92	97.9 $\pm$ 213	50.06 $\pm$ 149.06
Tyrrhenian	4.582	1.168	Non-significant	1.634		45.4 $\pm$ 161	30.6 $\pm$ 121	31.8 $\pm$ 154	89.6 $\pm$ 238	49.42 $\pm$ 175.50
LPC	2.558	1.316	Non-significant	1.459		40.9 $\pm$ 169	35.0 $\pm$ 134	30.8 $\pm$ 121	83.4 $\pm$ 234	47.58 $\pm$ 171.53
Ionian	Non-significant	Non-significant	Non-significant	Non-significant		45.6 $\pm$ 115	14.5 $\pm$ 59	16.1 $\pm$ 60	66.6 $\pm$ 132	35.70 $\pm$ 99.55
Levantine	Non-significant	Non-significant	Non-significant	Non-significant		47.1 $\pm$ 118	9.2 $\pm$ 40	2.3 $\pm$ 14	45.8 $\pm$ 109	26.05 $\pm$ 85.59
Aegean	-3.340	Non-significant	Non-significant	-1.707		64.8 $\pm$ 256	19.2 $\pm$ 86	10.8 $\pm$ 57	73.0 $\pm$ 227	41.92 $\pm$ 180.42
Adriatic	5.595	2.195	Non-significant	4.764		49.3 $\pm$ 174	41.6 $\pm$ 149	42.7 $\pm$ 146	83.9 $\pm$ 233	54.44 $\pm$ 180.01
BlackSea	2.820	Non-significant	Non-significant	2.738		58.1 $\pm$ 153	41.0 $\pm$ 95	42.4 $\pm$ 90	79.2 $\pm$ 155	55.21 $\pm$ 127.61

Table 2. Continued.

	Maximum mm month <sup>-1</sup> (yr)				Minimum mm month <sup>-1</sup> (yr)			
	Winter	Spring	Summer	Autumn	Winter	Spring	Summer	Autumn
Med	71.8 (2009)	29.6 (2002)	28 (2002)	87.4 (2008)	29.2 (2002)	9.5 (1999)	11.7 (2004)	55.3 (2006)
Active Atlantic Mediterranean	107 (2010)	27.8 (2008)	20.8 (2008)	98.6 (2010)	10.7 (2000)	2.7 (2005)	1.2 (2004)	21.1 (1998)
Alboran	151.3 (2010)	39 (2002)	18.6 (2008)	122.1 (2008)	9.5 (2000)	3.2 (2005)	1.1 (2003)	18.2 (1998)
Algerian	94.6 (2003)	49.9 (1998)	38.7 (2008)	132.6 (2010)	7.3 (2000)	10.7 (2005)	9.8 (2004)	63.4 (2009)
Tyrrhenian	111.8 (2010)	46.5 (2010)	60.7 (1998)	128.4 (2008)	15.4 (2002)	12.5 (2006)	17.3 (2004)	59 (2001)
LPC	96.9 (2010)	72.2 (2002)	54 (2002)	137.5 (2008)	12.9 (2005)	7 (2006)	17.3 (2004)	52.8 (2006)
Ionian	75.7 (2009)	20.4 (2007)	31.4 (2009)	87.4 (2007)	24.8 (2002)	4.9 (1999)	4.7 (2001)	51.2 (2000)
Levantine	65.7 (2003)	15.5 (1998)	6.5 (2009)	80.8 (2001)	34.1 (2001)	5.8 (2004)	0.2 (2004)	19.3 (1999)
Aegean	118.6 (1998)	29.6 (1998)	30.8 (2002)	126.1 (1998)	30.9 (2007)	8.4 (2005)	1.8 (2000)	46.8 (2008)
Adriatic	98 (2009)	60.5 (2009)	76.3 (2002)	128.1 (2009)	10.6 (1998)	19.5 (1998)	20.4 (1999)	37.4 (1999)
Black Sea	114.6 (2010)	63.3 (2010)	58.7 (2008)	114.1 (2007)	34.1 (2007)	20.4 (2003)	28.9 (2003)	42.7 (2000)



**Figure 4.** Annual precipitation time series for the ten studied sub-basins, calculated based on three-hour gridded TRMM data (AAM = Active Atlantic Mediterranean sub-basin west of the Strait of Gibraltar, Med = only the Mediterranean Sea).

### 3.2. Mediterranean sub-basin precipitation rate characteristics

In this section, time series are used to reveal the precipitation variation among the ten studied sub-basins, all of which display annual trends, ranging from  $3.46 \text{ mm month}^{-1} \text{ yr}^{-1}$  over the Adriatic sub-basin to  $-1.14 \text{ mm month}^{-1} \text{ yr}^{-1}$  over the Aegean sub-basin (Fig. 4 and Tab. 2).

The ten studied sub-basins display an annual average PR of approximately  $28.36 \text{ mm month}^{-1}$ , ranging from  $26.05 \text{ mm month}^{-1}$  in the Levantine sub-basin to  $54.4 \text{ mm month}^{-1}$  in the Adriatic sub-basin. This is also in accordance with previous findings of Shaltout and Omstedt (2014), who found that, in the Med+ region, the SST was lowest in the Levantine sub-basin. The negative relation between SST and PR is discussed in the next section.

The annual variation in PRs can also be illustrated by calculating the variance (Fig. 5). The figure illustrates that most of the studied stations are out of phase, indicating that the processes affecting precipitation differ between sub-basins. The only exception is between the LPC, Algerian, and Tyrrhenian sub-

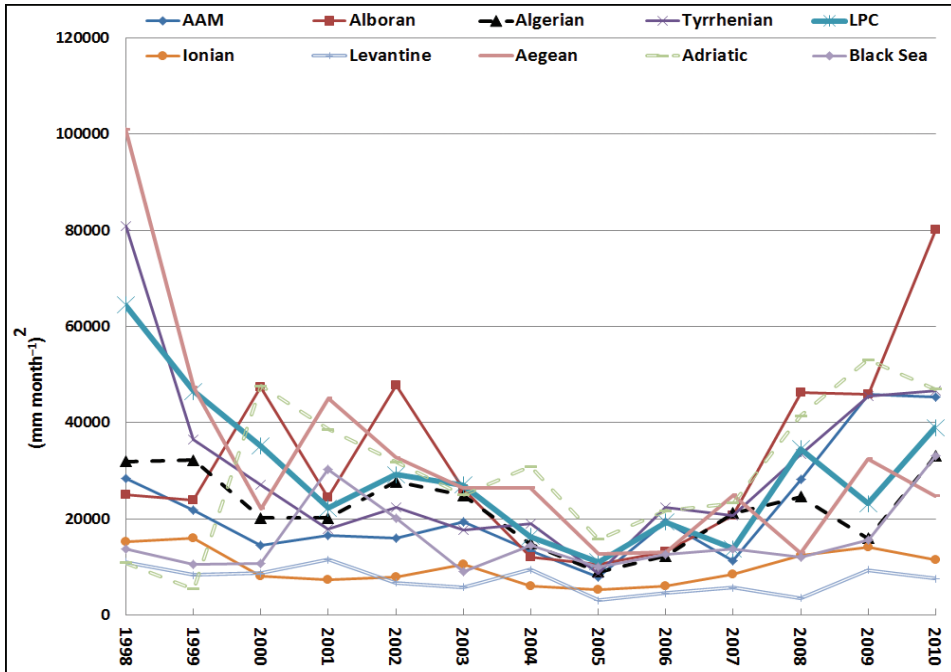


**Figure 5.** Annual precipitation variance for the ten studied sub-basins, calculated based on three-hour gridded TRMM data (AAM = Active Atlantic Mediterranean sub-basin west of the Strait of Gibraltar).

basins (correlation coefficient of annual variance between each two of them,  $R > 0.8$ ; number of observations,  $n = 13$ ; significance level  $> 99\%$ ).

Generally, the annual average total numbers of very wet days (i.e., over  $3.4 \text{ mm day}^{-1}$  of precipitation) in the study area range from 25.5 days over the Levantine sub-basin to 61.8 days over the Black Sea (Tab. 3). The Black Sea reaches its maximum number of very wet days in autumn at 26.7% of season days and its minimum number of very wet days in spring at 10.4% of season days. In contrast, the number of very wet days over the Levantine sub-basin ranges from 1.3% to 12.5% in spring and autumn, respectively.

### 3.3. Correlation between Mediterranean precipitation and atmospheric parameters

In most of the Med+ region, precipitation is not significantly correlated with the studied atmospheric parameters. However, in the northern Mediterranean Sea, precipitation is anti-correlated with SLP, especially in winter and spring (see Fig. 6), possibly due to the influence of the Alps. The Alps are believed to be a significant source of northern Mediterranean moisture transport (Lionello et

Table 3. Average annual numbers of very wet days defined as precipitation rates higher than  $3.4 \text{ mm day}^{-1}$  (Med = only the Mediterranean Sea, LPC = the Liguro-Provençal and Catalan sub-basins).

	Annual	Winter	Spring	Summer	Autumn
Med	38.3	10.5	2.5	2.5	22.8
Active Atlantic Mediterranean	28.2	9.5	3.2	1.2	14.5
Alboran	30.2	11.0	4.2	1.8	13.2
Algerian	53.8	12.2	8.8	6.5	26.2
Tyrrhenian	48.2	10.5	7.7	7.2	22.8
LPC	46.4	9.9	8.4	7.8	20.3
Ionian	37.5	11.0	2.2	4.2	20.2
Levantine	25.5	12.8	1.2	0.2	11.2
Aegean	39.5	14.3	3.8	2.4	19.0
Adriatic	53.2	11.3	9.9	10.9	21.0
Black Sea	61.8	16.2	9.4	12.2	24.0

al., 2006b) and the amount of moisture is greatly affected by SLP (Efthymiadis et al., 2007).

In the southern Mediterranean Sea, precipitation is directly correlated with SLP, especially over the north Levantine sub-basin in summer. This may be explained by the inverse effect of SLP on SST, i.e., high-pressure systems are associated with low SST, and low SST is associated with Mediterranean high stratiform precipitation as described by Trenberth and Shea (2005), Mariotti and Dell'Aquila (2012), Berg et al. (2013) and Shaltout and Omstedt (2014).

There is an inverse (direct) correlation between NAO and precipitation especially in winter (summer) in the north Tyrrhenian (north-east Ionian) sub-basin. Previous studies (e.g., Hurrell, 1995; Mariotti et al., 2002; Romanou et al., 2010) have demonstrated that precipitation in the Mediterranean Sea region is inversely correlated with the winter NAO over the western and north-central Mediterranean regions. However, the current study found that the NAO and precipitation are only correlated over the north Tyrrhenian sub-basin and the Black Sea. This disagreement could be due to the better resolution and improved accuracy of the TRMM database or due to the relatively short data period used for the current study. The sensitivity of the correlation to the time period using a few sub periods of TRMM data (1998–2006, 2000–2008 and 2000–2010) shows that the correlation is dependent on time especially during autumn and summer season. In autumn, PR is significantly monthly correlated with NAO over 10%, 8.7% and 15.4% of the Mediterranean Sea during the respective periods 1998–2006, 2002–2008 and 2002 and 2010. In summer, the monthly significant cor-

relation between PR and NAO is ranged from 24.5% for the period 2002–2010 to 2.5 % for the period 1998–2006.

SST is anti-correlated with precipitation throughout the study area, with the maximum inverse correlation occurring in spring and in the Levantine sub-basin (Fig. 6). This is also in good agreement with the previous finding from Trenberth and Shea, (2005), Mariotti and Dell’Aquila (2012), Berg et al. (2013) and Shaltout and Omstedt (2014). The findings of Berg et al. (2013) that the connective precipitation increase with increased temperature merits our interest and will be discussed in our future work.

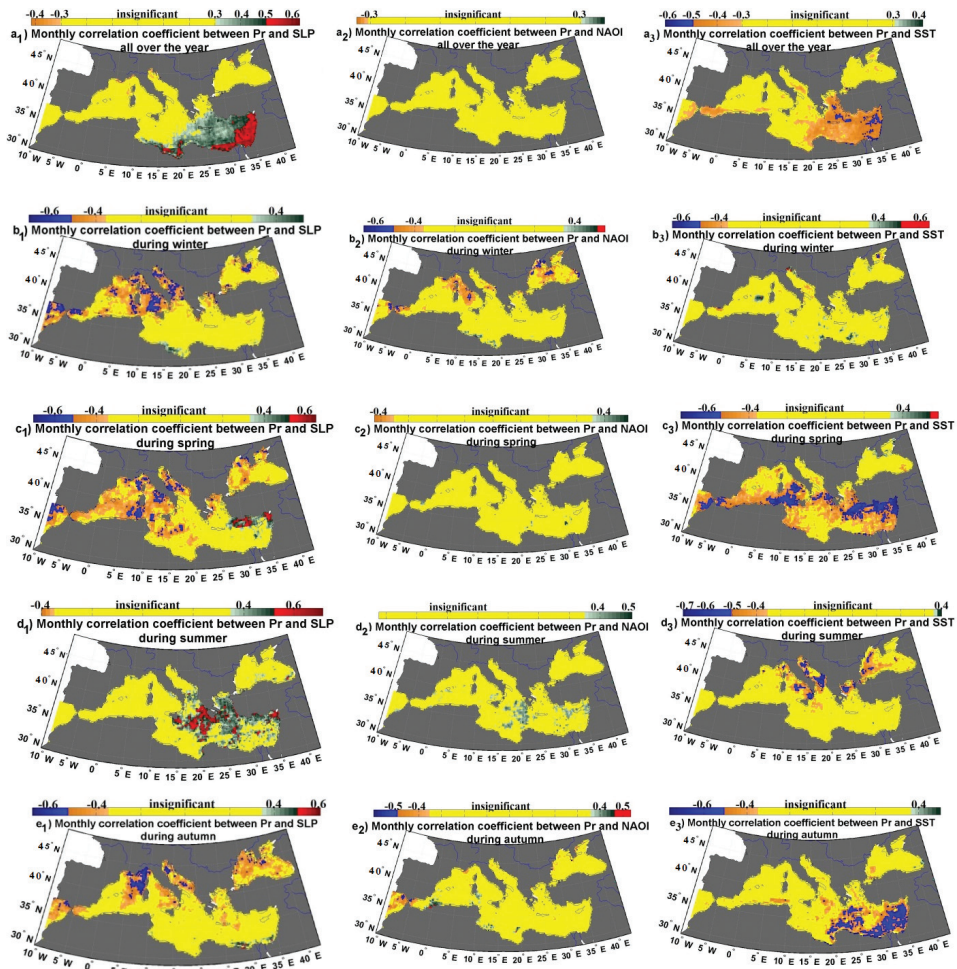


**Figure 6.** Annual and seasonal correlation coefficients between precipitation over the Mediterranean Sea and adjacent sub-basins and the studied atmospheric components.

### 3.4. Scenario calculations

In this section, the future PRs of the Med+ region projected until 2100 are investigated using the results of six GCM models and with four scenarios, i.e., RCP26, RCP45, RCP60, and RCP85. Five of the GCMs used are available based on only one set of initial conditions; however, the CCSM4 GCM is available with six initial conditions (realizations).

#### 3.4.1. Present conditions based on the control period, 1998–2010

The performances of the various GCM realizations for the RCP26 and RCP85 emission scenarios over the Med+ region are shown in Tab. 4. The results for scenarios RCP45 and RCP60 are not shown, as they are quite similar. In Tab. 4, the PR results obtained using the TRMM data and different GCM realizations are tested for significance using *t*-tests (significance level = 95%).

The models that best describe precipitation of the Med+ region during the control period are GFDL-CM3-1, MIROC-ESM-CHEM, and HadGEM2-AO, in comparison with TRMM data. The GFDL-CM3-1 and MIROC-ESM-CHEM models underestimate PRs by approximately  $-14\%$  ( $-16\%$ ) and  $-8\%$  ( $-5\%$ ), respectively, during scenario RCP26 (RCP85). However, the HadGEM2-AO model overestimates the Med+ region PRs by approximately  $19\%$  ( $16\%$ ) during scenario RCP26 (RCP85).

Mini-ensemble means (EMR3) based on three GCMs (i.e., GFDL-CM3-1, MIROC-ESM-CHEM, and HadGEM2-AO) are calculated and presented in the last row for each scenario in Tab. 4. The annual EMR3 displays negligible bias for the PRs of the Med+ region. However, EMR3 displays large seasonal biases, particularly in spring and autumn. Generally, EMR3 scenarios result in estimated PRs that best describe the control period (Tab. 4), and this mini-ensemble mean will be used to analyse future changes and uncertainties in the PRs in next section.

#### 3.4.2. Future Mediterranean Sea precipitation change, 2000–2100

The mini-ensemble calculations based on the mean of three GCMs (EMR3) indicate a significant drought over the current century in the Med+ region, the maximum (minimum) drought being based on calculations using scenario RCP85 (RCP26) (Fig. 7a and Tab. 5). The change in the PRs of the Med+ region by the end of the current century is comparable to the PRs at first part of the current century, the change ranging from no change to a precipitation reduction of  $7.5 \text{ mm month}^{-1}$ ; in the AAM sub-basin the precipitation change ranges from  $-2.7$  to  $-9.5 \text{ mm month}^{-1}$  and in the Black Sea from insignificant change to  $-4.5 \text{ mm month}^{-1}$ .

The AAM sub-basin displays the strongest drying trends, stronger than those of the Mediterranean and Black seas. The Mediterranean Sea displays spatial variability in drying trends between its various sub-basins, the maximum (min-

Table 4. Performance of various studied GCMs over the Mediterranean Sea in the control period (1998–2010) during scenarios RCP26, and RCP85. Model CCSM4 is available with six initial conditions. Gray shading indicates the GCMs that best describe the precipitation rates during the control period. EMR3 = ensemble mean of the three models that best describe the present Mediterranean Sea precipitation, i.e., models GFDL-CM3-1, MIROC-ESM-CHEM, and HadGEM2-AO models. Bias =  $\% \frac{GCM - TRMM PR}{TRMM PR}$ .

Scenario		Model	Winter	Spring	Summer	Autumn	Annual
Precipitation (Bias = %)	RCP26	bcc-csm1-1	-19.8	-17.6	-14.4	-29.3	-23.2
		GFDL-CM3-1	-7.9	47.2	-15.5	-36.4	-14.2
		MRI-CGCM3	-33.8	-8.2	34.5	-24.3	-18.4
		MIROC-ESM-CHEM	-10.8	43.8	22.8	-28.5	-7.7
		HadGEM2-AO	25.4	16.7	-2.9	21.7	19.4
		CCSM4_000	-22.0	-12.6	-48.3	-34.1	-29.2
		CCSM4_001	-12.5	-23.7	-37.0	-33.9	-26.4
		CCSM4_002	-20.7	-17.0	-47.4	-34.1	-29.2
		CCSM4_003	-18.2	-11.1	-48.9	-31.2	-26.6
		CCSM4_004	-30.8	-14.4	-36.0	-32.2	-29.8
	CCSM4_005	-32.1	-25.0	-46.8	-30.3	-32.0	
	EMR3	2.2	35.9	1.5	-14.4	-0.8	
	RCP85	bcc-csm1-1	-20.6	-21.2	-15.1	-27.6	-23.2
		GFDL-CM3-1	-21.5	44.9	-11.4	-32.4	-16.4
		MRI-CGCM3	-30.2	-4.7	21.2	-19.5	-16.1
		MIROC-ESM-CHEM	-7.0	47.1	26.7	-27.7	-5.3
		HadGEM2-AO	20.9	13.0	-6.1	19.5	16.2
		CCSM4_000	-24.4	-11.2	-42.8	-26.9	-25.8
CCSM4_001		-17.7	-20.1	-30.2	-28.8	-24.5	
CCSM4_002		-17.3	-20.4	-46.8	-34.5	-28.8	
CCSM4_003		-22.4	-10.6	-45.3	-36.4	-29.7	
CCSM4_004		-28.2	-9.6	-41.9	-28.0	-27.1	
CCSM4_005	-26.3	-17.6	-41.5	-30.6	-28.8		
EMR3	-2.5	35.0	3.0	-13.5	-1.8		

imum) drying trends occurring in the Aegean sub-basins (the Alboran, Tyrrhenian, and LPC sub-basins), as seen in Tab. 5.

Generally, there is strong variability in the seasonal drought projections (Fig. 7b and Tab. 5). The only exception to the reduced PRs is the positive winter trend for the Black Sea (Tab. 5). The Mediterranean Sea PRs are projected to lead to droughts in each scenario, most pronounced in winter and less pronounced in summer and spring, as seen in Tab. 5. Current results support the study of Giorgi and Lionello (2008) and IPCC (2013).

Table 5. Change in the EMR3 calculated precipitation rates ( $\text{mm month}^{-1}$ ) in the various sub-basins at the end of the 21<sup>st</sup> century (relative to precipitation rates, 2000–2029) for the four studied RCP scenarios.

Sub-basin	RCP	Winter	Spring	Summer	Autumn	Annual
Med	RCP26	0.1	-0.1	-1.3	0.2	-0.2
	RCP45	-3.0	-2.1	-2.4	-6.3	-3.5
	RCP60	-3.9	-2.3	-2.7	-4.8	-3.7
	RCP85	-9.1	-5.8	-5.8	-8.4	-7.5
AAM	RCP26	-4.1	-3.8	1.1	-4.0	-2.7
	RCP45	-4.8	-7.5	-0.2	-11.1	-5.9
	RCP60	-9.6	-9.7	1.2	-11.6	-7.1
	RCP85	-12.7	-8.6	1.1	-17.6	-9.5
Black Sea	RCP26	4.4	0.8	-2.7	-2.8	-0.2
	RCP45	7.4	2.3	-5.2	2.3	1.6
	RCP60	4.8	2.3	-6.4	1.7	0.6
	RCP85	1.8	-2.8	-10.9	-6.1	-4.5
Alboran	RCP26	-3.7	-2.4	1.6	-1.5	-1.5
	RCP45	-4.1	-6.6	0.3	-5.6	-3.8
	RCP60	-6.4	-6.7	1.7	-4.2	-3.9
	RCP85	-7.6	-9.6	2.2	-9.5	-6.2
Algerian	RCP26	-1.0	1.1	-1.8	0.2	-0.3
	RCP45	-2.9	-2.6	-2.1	-8.2	-3.9
	RCP60	-7.6	-4.1	-1.6	-5.0	-4.5
	RCP85	-11.0	-7.1	-1.3	-7.9	-7.1
Tyrrhenian	RCP26	-0.9	1.3	-3.0	1.0	-0.4
	RCP45	-0.7	-1.9	-2.3	-7.0	-3.1
	RCP60	-3.1	-2.4	-3.7	-3.4	-3.5
	RCP85	-6.8	-5.7	-8.2	-4.2	-6.4
LPC	RCP26	3.7	3.1	-2.5	2.1	1.7
	RCP45	1.0	-0.9	-3.9	-8.4	-3.1
	RCP60	-2.4	-3.7	-2.0	-1.3	-2.2
	RCP85	-4.2	-8.2	-11.0	-2.1	-6.4
Ionian	RCP26	0.3	-0.7	-1.4	1.4	0.0
	RCP45	-4.9	-3.0	-1.8	-4.8	-3.7
	RCP60	-4.3	-2.6	-3.0	-5.6	-4.2
	RCP85	-10.9	-4.3	-4.1	-6.9	-7.0
Levantine	RCP26	-0.7	-1.0	-0.1	1.2	-0.2
	RCP45	-4.0	-1.2	-0.8	-6.6	-3.0
	RCP60	-2.9	-1.7	-0.3	-7.6	-3.4
	RCP85	-9.2	-3.7	-1.1	-14.1	-7.3
Aegean	RCP26	0.1	-3.8	-2.0	-6.1	-2.7
	RCP45	-3.1	-2.8	-6.3	-5.5	-4.4
	RCP60	-1.3	-0.4	-6.1	-5.8	-3.8
	RCP85	-10.2	-8.8	-8.7	-16.2	-11.2
Adriatic	RCP26	-1.2	1.7	-1.3	-3.2	-0.9
	RCP45	-0.7	-1.1	-4.3	-7.6	-3.6
	RCP60	-4.6	0.3	-7.2	1.7	-2.8
	RCP85	-8.6	-7.8	-20.2	-3.8	-10.1

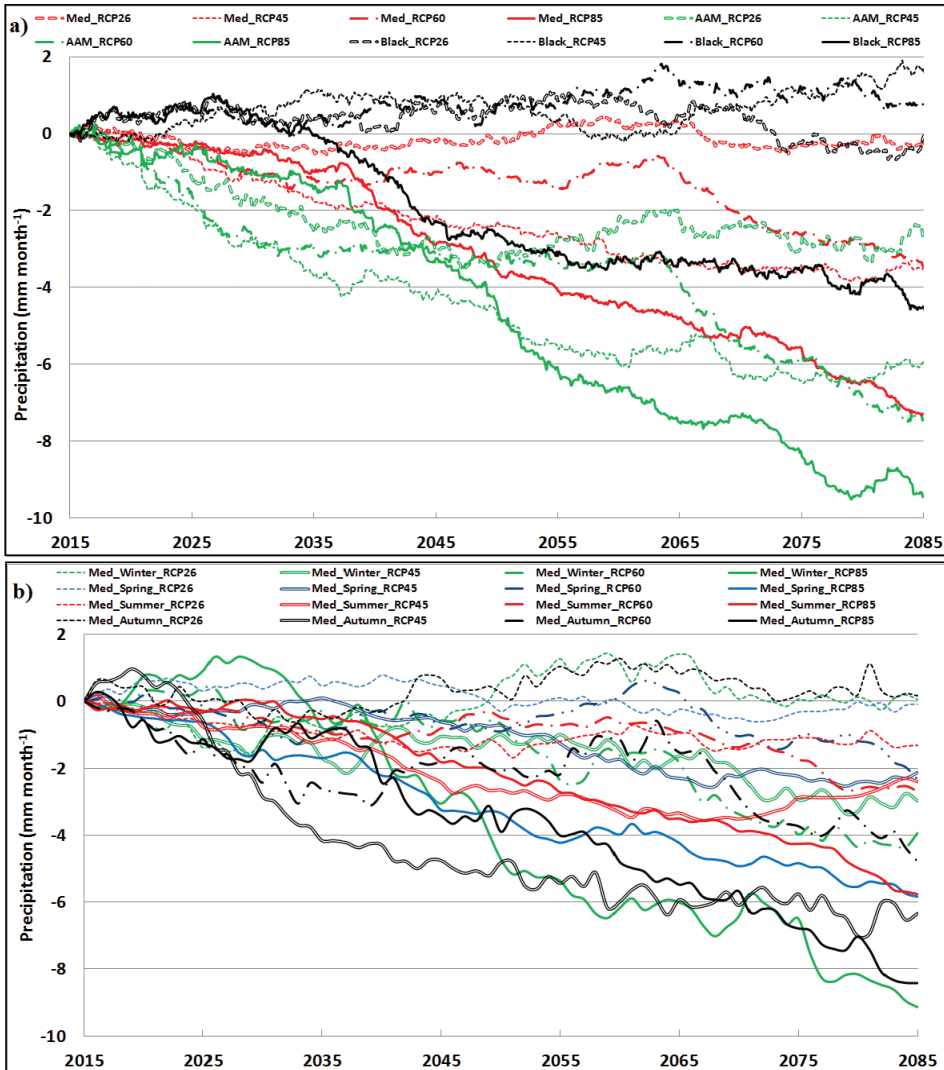


**Figure 7.** Thirty-year running (a) annual and (b) seasonal PR means with reference to the 2000–2029 period for the EMR3 (EMR3 = Ensemble-mean realizations based on the GCMs that best describe the current PR, i.e., the GFDL-CM3-1, MIROC-ESM-CHEM, and HadGEM2-AO models).

### 3.5. Uncertainty measurements

In this study, four sources of uncertainty are taken into consideration: uncertainty associated with the scenarios, the GCMs, seasonal variations, and regional variations. The uncertainty due to the GCMs used was taken into account by calculating the ensemble of GCMs (Hagemann et al., 2012). In the

current paper, the impact of GCM-related uncertainty is discussed only for the models used in the mini-ensemble simulation.

Uncertainties in the PRs projected for the Med+ region at the end of the current century were estimated to be 7.3, 4.5, 3.2, and 2.8 mm month<sup>-1</sup> due to the scenario used, GCM used, regional variations, and seasonal variations, respectively. The greatest estimated uncertainty originates from the particular emission scenario used. Overall, the projected PRs are affected by a wide range of uncertainties, calling for various assumptions regarding future socioeconomic adaptation measures. Questions such as: How should uncertainty, risk, and precaution be incorporated into effective ocean governance and policy-making? merit considerable future attention but will not be addressed here.

#### 4. Discussion and conclusion

Precipitation in the Mediterranean Sea and adjacent regions during the 1998–2010 period is affected by sea surface temperature and large-scale sea level pressure but only in parts of the system, and NAO has a small effect. This indicates that the studied PRs are largely controlled by the regional meteorology.

Recent remote sensing TRMM precipitation data indicate a range of drought and wetter events in the studied region, while ensemble mean scenarios indicate decreasing PRs over the present century.

The Mediterranean Sea and adjacent regions received an average annual precipitation of  $39.4 \pm 65$  mm month<sup>-1</sup> over the 13 years from 1998 to 2010, ranging from  $47.7 \pm 72$  mm month<sup>-1</sup> in winter to  $17.5 \pm 37$  mm month<sup>-1</sup> in summer. The Black Sea (AAM sub-basin) had higher (lower) PRs. These calculations are in accordance with previous calculations by Mariotti et al. (2002), Romanou et al. (2010), and Shaltout and Omstedt (2012). In addition, the current PRs in the studied area indicate a wetting trend of 0.9 mm month<sup>-1</sup> yr<sup>-1</sup> with seasonal variability peaking at 1 mm month<sup>-1</sup> yr<sup>-1</sup> in winter. The Black Sea and AAM sub-basin display stronger current wetting trends. The current Mediterranean Sea precipitation trend is not uniform, as some sub-basins display drying trends (e.g., the Aegean sub-basin), while others display no change (e.g., the Ionian and Levantine sub-basins), or wetting trends (e.g., the Alboran sub-basin). This is in contrast to Romanou et al.'s (2010) results, probably due to the different periods and databases studied. Moreover, the current Mediterranean Sea precipitation rates are dependent on the study period and the period 2005–2009 represent the maximum wetting trend over the 1998–2010 years.

Future PRs (CMIP5 scenarios) over the study period were described using mini-ensemble mean of the GCMs that best describe the current PRs. Based on direct comparison between TRMM precipitation data and the results of various GCM realizations, the GFDL-CM3-1, MIROC-ESM-CHEM, and HadGEM2-AO models were found to be closest to the TRMM data. Mini-ensemble mean realiza-

tions calculated based only on these three GCMs display negligible biases compared with the TRMM data. The mini-ensemble mean realizations were then used to project future PRs during the 21<sup>st</sup> century.

During the 21<sup>st</sup> century, the general projected decline in the annual Mediterranean PR was  $-7.5 \text{ mm month}^{-1} \text{ century}^{-1}$  under scenario RCP85; however, the Black Sea (AAM sub-basin) displays a weaker (stronger) drying trend. The drying trends projected for the Mediterranean Sea and adjacent areas over the 21<sup>st</sup> century were not uniform, as some sub-basins under certain scenarios displayed wetting trends (e.g., the LPC sub-basin under scenario RCP26 and the Black Sea under scenario RCP45) while other sub-basins displayed negligible trends (e.g., the Mediterranean Sea under scenario RCP26). This is in agreement with earlier findings of Giorgi and Lionello (2008). The variation in PRs projected for the 21<sup>st</sup> century was dominated by emission variations and not by used GCMs or regional or seasonal variations, indicating that management efforts should emphasize emission reductions. This is in agreement with previous findings of Shaltout and Omstedt (2014).

Generally, more droughts can be expected for the Mediterranean Sea and adjacent regions, as addressed here, together with warming trends (Shaltout and Omstedt, 2014). These changes are in consistent with IPCC (2013) and will greatly affect the water and heat balances of the Mediterranean Sea and therefore the Sea's salinity and temperatures. Climate change may thus have an impact on several aspects, such as sea levels, Mediterranean Sea outflow, and Mediterranean marine ecosystems, aspects that merit further research.

*Acknowledgements* – This research was undertaken when Dr. Mohamed Shaltout was a visiting scientist at the Ocean Climate Group, Department of Earth Sciences, University of Gothenburg, Sweden. We would like to thank Dr. Riccardo Farneti at Earth System Physics Section, ICTP, Trieste, Italy, for his valuable comments. We would also like to thank Stephen Sanborn at Proper English AB for the English language editing.

## References

- Baek, H., Lee, J., Lee, H., Hyun, Y., Cho, C., Kwon, W., Marzin, C., Gan, S., Kim, M., Choi, D., Lee, J., Lee, J., Boo, K., Kang, H. and Byun, Y. (2013): Climate change in the 21st century simulated by HadGEM2-AO under representative concentration pathways, *Asia-Pacific J. Atmos. Sci.*, **49**, 603–618, DOI: [10.1007/s13143-013-0053-7](https://doi.org/10.1007/s13143-013-0053-7).
- Berg, P., Moseley, C. and Haerter, J. (2013): Strong increase in convective precipitation in response to higher temperatures, *Nat. Geosci.*, **6**, 181–185, DOI: [10.1038/ngeo1731](https://doi.org/10.1038/ngeo1731).
- Bordi, I. and Sutera, A. (2008): Drought over Europe in recent years, *Options Méditerranéennes (Series A)*, **80**, 63–68, available at <http://om.ciheam.org/om/pdf/a80/00800420.pdf>
- Chou, C. and Lan, C. (2012): Changes in the annual range of precipitation under global warming, *J. Climate*, **25**, 222–235, DOI: [10.1175/JCLI-D-11-00097.1](https://doi.org/10.1175/JCLI-D-11-00097.1).
- Donner, J., Wyman, B., Hemler, R., Horowitz, L., Ming, Y., Zhao, M., Golaz, J., Ginoux, P., Lin, S., Schwarzkopf, M., Austin, J., Alaka, G., Cooke, W., Delworth, T., Freidenreich, S., Gordon, C., Griffies, S., Held, I., Hurlin, W., Klein, S., Knutson, T., Langenhorst, A. Lee, H., Lin, Y., Magi, B., Malyshev, S., Milly, P., Naik, V., Nath, M., Pincus, R., Ploshay, J., Ramaswamy, V., Seman,

- C., Shevliakova, E., Sirutis, J., Stern, W., Stouffer, R., Wilson, R., Winton, M., Wittenberg, A. and Zeng, F. (2011): The dynamical core, physical parameterizations, and basic simulation characteristics of the atmospheric component AM3 of the GFDL Global Coupled Model CM3, *J. Climate*, **24**, 3484–3519, DOI: [10.1175/2011JCLI3955.1](https://doi.org/10.1175/2011JCLI3955.1).
- Efthymiadis, D., Jones, P., Briffa, K., Böhm, R. and Maugeri, M. (2007): Influence of large-scale atmospheric circulation on climate variability in the Greater Alpine Region of Europe, *J. Geophys. Res.*, **112**, D12104, DOI: [10.1029/2006JD008021](https://doi.org/10.1029/2006JD008021).
- Gent, P., Danabasoglu, G., Donner, L., Holland, M., Hunke, E., Jayne, S., Lawrence, D., Neale, R., Rasch, P., Vertenstein, M., Worley, P., Yang, Z. and Zhang, M. (2011): The community climate system model Version 4, *J. Climate*, **24**, 4973–4991, DOI: [10.1175/2011JCLI4083.1](https://doi.org/10.1175/2011JCLI4083.1).
- Giorgi, F. and Lionello, P. (2008): Climate change projections for the Mediterranean region, *Global Planet. Change*, **63**, 90–104, DOI: [10.1016/j.gloplacha.2007.09.005](https://doi.org/10.1016/j.gloplacha.2007.09.005).
- Gopalan, K., Wang, N., Ferraro, R. and Liu, C. (2010): Status of the TRMM 2A12 land precipitation algorithm, *J. Atmos. Oceanic Technol.*, **27**, 1343–1354, DOI: [10.1175/2010JTECHA1454.1](https://doi.org/10.1175/2010JTECHA1454.1).
- Hagemann, S., Chen, C., Clark, D. B., Folwell, S., Gosling, S. N., Haddeland, I., Hanasaki, N., Heinke, J., Ludwig, F., Voß, F. and Wiltshire, A. J. (2012): Climate change impact on available water resources obtained using multiple global climate and hydrology models, *Earth Syst. Dynam. Discuss.*, **3**, 1321–1345, DOI: [10.5194/esd-4-129-2013](https://doi.org/10.5194/esd-4-129-2013).
- Henry, P. (1977): The Mediterranean: A threatened microcosm, *Ambio*, **6**, 300–307.
- Huffman, G. J., Adler, R. F., Bolvin, D. T., Gu, G., Nelkin, E.J., Bowman, K. P., Hong, Y., Stocker, E. F. and Wolff, D. B. (2007): The TRMM multi-satellite precipitation analysis: Quasi-global, multi-year, combined-sensor precipitation estimates at fine scale, *J. Hydrometeor.*, **8**, 38–55, DOI: [10.1175/JHM560.1](https://doi.org/10.1175/JHM560.1).
- Hurrell, J. W. (1995): Decadal trends in the North Atlantic Oscillation: Regional temperature and precipitation, *Science*, **269**, 676–679, DOI: [10.1126/science.269.5224.676](https://doi.org/10.1126/science.269.5224.676).
- Intergovernmental Panel on Climate Change (IPCC) (2013): Summary for Policymakers, in *Climate Change 2013: The Physical Science Basis. Contribution of Working Group I to the Fifth Assessment Report of the Intergovernmental Panel on Climate Change* edited by Stocker, T. F., D. Qin, G.-K. Plattner, M. Tignor, S. K. Allen, J. Boschung, A. Nauels, Y. Xia, V. Bex and P. M. Midgley. Cambridge University Press, Cambridge, United Kingdom and New York, NY, USA.
- Jacobeit, J., Dünkeloh, A. and Hertig, E. (2007): Mediterranean rainfall changes and their causes, in *Global change: Enough water for all?*, edited by Lozán J. L., H. Graß, P. Hupfer, L. Menzel, and C.-D. Schönwiese, Wissenschaftliche Auswertungen, Hamburg, Germany, 195–199.
- Kelley, C., Ting, M., Seager, R. and Kushnir, Y. (2012): Mediterranean precipitation climatology, seasonal cycle, and trend as simulated by CMIP5, *Geophys. Res. Lett.*, **39**, L21703, DOI: [10.1029/2012GL053416](https://doi.org/10.1029/2012GL053416).
- Kjellström, E. M., Grigory, N., Hansson, U., Strandberg, G. and Ullerstig, A. (2011): 21st century changes in the European climate: Uncertainties derived from an ensemble of regional climate model simulations, *Tellus*, **63A**, 24–40, DOI: [10.1111/j.1600-0870.2010.00475.x](https://doi.org/10.1111/j.1600-0870.2010.00475.x).
- Lionello, P., Malanotte-Rizzoli, P., Boscolo, R., Alpert, V., Artale, L., Li, J., Luterbacher, J., May, W., Trigo, R., Tsimplis, M., Ulbrich, U. and Xoplaki, E. (2006a): The Mediterranean climate: An overview of the main characteristics and issues, in *Mediterranean Climate Variability* edited by Lionello, P., Malanotte-Rizzoli, P. and Boscolo, R., Elsevier, Amsterdam, 1–26, DOI: [10.1016/S1571-9197\(06\)80003-0](https://doi.org/10.1016/S1571-9197(06)80003-0).
- Lionello, P., Bhend, J., Buzzi, A., Della-Marta, P. M., Krichak, S. O., Jansa, A., Maheras, P., Sanna, A., Trigo, I. F. and Trigo, R. (2006b): Cyclones in the Mediterranean region: Climatology and effects on the environment, in *Mediterranean Climate Variability*, edited by Lionello, P., Malanotte-Rizzoli, P. and Boscolo, R., Elsevier, Amsterdam, 325–372, DOI: [10.1016/S1571-9197\(06\)80009-1](https://doi.org/10.1016/S1571-9197(06)80009-1).
- Mariotti, A. and Dell'Aquila, A. (2012): Decadal climate variability in the Mediterranean region: roles of large-scale forcings and regional processes, *Clim. Dyn.*, **38**, 1129–1145, DOI: [10.1007/s00382-011-1056-7](https://doi.org/10.1007/s00382-011-1056-7).

- Mariotti, A., Struglia, M., Zeng, N. and Lau, K. (2002): The hydrological cycle in the Mediterranean region and implications for the water budget of the Mediterranean Sea, *J. Climate*, **15**, 1674–1690, DOI: 10.1175/1520-0442(2002)015<1674:THCITM>2.0.CO;2.
- Shaltout, M. and Omstedt, A. (2012): Calculating the water and heat balances of the Eastern Mediterranean Basin using ocean modelling and available meteorological, hydrological and ocean data, *Oceanologia*, **54**, 199–232, DOI: 10.5697/oc.54-2.199.
- Shaltout, M. and Omstedt, A. (2014): Recent sea surface temperature trends and future scenarios for the Mediterranean Sea, *Oceanologia*, **56**, 411–443, DOI: 10.5697/oc.56-3.411.
- Shaltout, M., El Gindy, A. and Omstedt, A. (2013): Recent climate trends and future scenarios in the Egyptian Mediterranean coast based on six global climate models, *Geofizika*, **30**, 19–41.
- Romanou, A., Tselioudis, G., Zerefos, C., Clayson, C., Curry, J. and Andersson, A. (2010): Evaporation-precipitation variability over the Mediterranean and the Black Seas from satellite and re-analysis estimates, *J. Climate*, **23**, 5268–5287, DOI: 10.1175/2010JCLI3525.1.
- Taylor, K. E., Stouffer, R. J. and Meehl, G. A. (2012): An overview of CMIP5 and the experiment design, *Bull. Amer. Meteor. Soc.*, **93**, 485–498, DOI: 10.1175/BAMS-D-11-00094.1.
- Tongwen, W., Li, W., Ji, J., Xin, X., Li, L., Wang, Z., Zhang, Y., Li, J., Zhang, F., Wei, M., Shi, X., Wu, F., Zhang, L., Chu, M., Jie, W., Liu, Y., Wang, F., Liu, X., Li, Q., Dong, M., Liu, Q. and Zhang, J. (2013): Global carbon budgets simulated by the Beijing Climate Center Climate System Model for the last century, *J. Geophys. Res. – Atmospheres*, **118**, 4326–4347, DOI: 10.1002/jgrd.50320.
- Trenberth, K. and Shea, D. (2005): Relationships between precipitation and surface temperature, *Geoph. Res. Lett.*, **32**, L14703, DOI: 10.1029/2005GL022760.
- Watanabe, S., Hajima, T., Sudo, K., Nagashima, T., Takemura, T., Okajima, H., Nozawa, T., Kawase, H., Abe, M., Yokohata, T., Ise, T., Sato, H., Kato, E., Takata, K., Emori, S. and Kawamiya, M. (2011): MIROC-ESM 2010: Model description and basic results of CMIP5-20c3m experiments, *Geosci. Model Dev.*, **4**, 845–872, DOI: 10.5194/gmd-4-845-2011.
- Xoplaki, E. (2002): *Climate variability over the Mediterranean*. PhD thesis, University of Bern, Switzerland, 193 pp, available at [http://sinus.unibe.ch/klimet/docs/phd\\_xoplaki.pdf](http://sinus.unibe.ch/klimet/docs/phd_xoplaki.pdf)
- Xoplaki, E., Gonzalez-Rouco, J., Luterbacher, J. and Wanner, H. (2004): Wet season Mediterranean precipitation variability: Influence of large-scale dynamics and trends, *Clim. Dyn.*, **23**, 63–78, DOI: 10.1007/s00382-004-0422-0.
- Yukimoto, S., Yoshimura, H., Hosaka, M., Sakami, T., Tsujino, H., Hirabara, M., Tanaka, T. Y., Deushi, M., Obata, A., Nakano, H., Adachi, Y., Shindo, E., Yabu, S., Ose, T. and Kitoh, A. (2011): Meteorological Research Institute – Earth System Model v1 (MRI-ESM1) – Model Description, *Technical Reports of the Meteorological Research Institute*, No. 64, ISSN 0386-4049, Meteorological Research Institute, Japan, 88 pp, available at [http://www.mri-jma.go.jp/Publish/Technical/DATA/VOL\\_64/index.html](http://www.mri-jma.go.jp/Publish/Technical/DATA/VOL_64/index.html)

## SAŽETAK

## Recentni trendovi oborine i budući scenariji nad Sredozemnim morem

Mohamed Shaltout i Anders Omstedt

U ovome radu analiziraju se aktualni intenziteti oborine (PR) i trendovi oborine nad područjem Sredozemnog mora i njihovi odzivi na scenarije općih klimatskih promjena. U analizi se koristi niz podataka intenziteta oborine u mreži od 0,25° tijekom 13-godišnjeg razdoblja (1998–2010) uzet iz podataka dobivenih daljinskim mjerenjima tijekom Misije mjerenja tropske oborine (Tropical Rainfall Measuring Mission, TRMM). Budući scenariji koriste rezultate iz šest općih klimatskih modela (globalni klimatski model, GCM)

uz četiri scenarija reprezentativnih staza koncentracije (RCP) (tj. RCP26, RCP45, RCP60 i RCP85).

Rezultati indiciraju da područje Sredozemnog mora pokazuje sezonski signifikantno (nesignifikantno) vlažniji trend tijekom hladnih (toplih) sezona, te tijekom promatranog razdoblja (1998–2010) prikazuje godišnju prostornu varijaciju koja se kreće u rasponu od 15 do preko 100 mm mjeseč<sup>-1</sup>. Tlak zraka na razini mora ima dva različita učinka na oborinu nad Sredozemljem. Nad sjevernim Sredozemljem obrnuto je razmjern oborini, dok je nad južnim Sredozemljem izravno razmjern oborini. Međutim, temperatura površine mora je antikorelirana s oborinom. Opći klimatski modeli koji najrealističnije opisuju aktualnu oborinu nad Sredozemljem su: GFDL-CM3-1, MIROC-ESM-CHEM i HadGEM2-AO, a koriste se za izračun srednjaka ansambla za svaki scenarij reprezentativne staze koncentracije. Realizacije srednjaka ansambla indiciraju da će područje studije doživjeti znatnu sušu u 21. stoljeću. Nesigurnost u projiciranoj oborini nad Sredozemnim morem pripisana je četirima izvorima, gdje je od njih najvažniji korišten scenarij.

*Ključne riječi:* Sredozemno more, Crno more, oborina, klimatski modeli

*Corresponding author's address:* Mohamed Shaltout, University of Alexandria, Faculty of Science, Department of Oceanography, Alexandria, Egypt, P. O. Box 460, 40 530 Gothenburg, Sweden; e-mail: mohamed.shaltot@alexu.edu.eg